Preprint
UCRL-JC-138889

Modeling and Mitigation of Stress Corrosion Cracking in Closure Welds of High-Level Waste Container for Yucca Mountain

J. Farmer, S. Lu, T. Summers, D. McCright, A. Lingenfelter,
F. Wang, J. Estill, L. Hackel, H.-L. Chen, G. Gordon, V. Pasupathi,
P. Andresen, S. Tang, M. Herrera

U.S. Department of Energy
Lawrence Livermore National Laboratory

This article was submitted to
2000 American Society of Mechanical Engineers, Pressure Vessels & Piping Conference, Seattle, Washington, July 23-27, 2000

May 12, 2000

American Society of Mechanical Engineers
Seattle, Washington – July 2000

MODELING AND MITIGATION OF STRESS CORROSION CRACKING IN CLOSURE WELDS OF HIGH-LEVEL WASTE CONTAINER FOR YUCCA MOUNTAIN

Joseph Farmer, Stephen Lu, Tammy Summers, Daniel McCright, Al Lingenfelter, Francis Wang, John Estill, Lloyd Hackel & Hao-Lin Chen
Lawrence Livermore National Laboratory
Livermore, California

Gerry Gordon & Venkataraman Pasupathi
Framatome-Cogema Fuels
Las Vegas, Nevada

Peter Andresen
General Electric Corporate Research and Development Center
Schenectady, New York

Stan Tang & Marcos Herrera
Structural Integrity Associates
San Jose, California

INTRODUCTION

EDA II Design Concept. As described in the License Application Design Selection Report, the recommended waste package design is Engineering Design Alternative II (CRWMS M&O 1999). This design includes a double-wall waste package (WP) underneath a protective drip shield (DS). A schematic representation of the WP is shown in Figure 1. The waste package outer barrier (WPOB) is to be made of Alloy 22 (UNS N06022), while the underlying structural support is to be made of 316NG or 316L (UNS S31603) (Treseder et al. 1991). Alloy 22 is a high-performance nickel-based alloy with substantial amounts of chromium (21%), molybdenum (13%) and tungsten (3%). The drip shield is to be made of Titanium Grade 7 (UNS R52400). This particular material contains palladium (0.12-0.25%) to enhance resistance to hydrogen induced cracking.

Stress Corrosion Cracking. There are several modes of failure that could lead to premature breach of the waste package. One of the most threatening is stress corrosion cracking (SCC). Initiation and propagation of SCC can occur at relatively low stress intensity factors (K_I). After initiation, through-wall penetration is essentially instantaneous when compared to the 10,000-year time scale of importance to the high-level waste repository at Yucca Mountain. Three criteria have to be met for SCC to occur: metallurgical susceptibility; a corrosive environment; and static tensile stresses. Environments that cause SCC are usually aqueous and can be condensed layers of moisture or bulk solutions. The SCC of a particular alloy is usually caused by the presence of a specific chemical species in the environment. For example, the SCC of copper alloys is virtually always due to the presence of ammonia in the environment. Chloride ions cause SCC in stainless steels and aluminum-based alloys. Reduced sulfate is known to promote SCC in nickel-based alloys. Changes in the environmental conditions, which include temperature, dissolved oxygen, and ionic concentrations, will normally influence the SCC process. Environmental conditions believed to be relevant to Yucca Mountain are described in the companion paper entitled *General and Localized Corrosion of Outer Barrier of High-Level Waste Container in Yucca Mountain.* Plausible conditions are represented by several standardized test media which include simulated dilute water (SDW), simulated concentrated water (SCW), simulated acidified water (SAW), simulated saturated water (SSW), and basic saturated water (BSW). These solutions are based upon the concentration of J-13 well water (Harrar et al. 1999). Radionuclide release is possible if SCC causes breach of the WPOB and underlying structural support. Adequate models to account for SCC must therefore be employed. As will be discussed subsequently, the highest stress in the WPOB (and the highest probability of SCC) will be in the final closure weld. The ring-core technique has been used to quantify the residual tensile stress in Alloy 22 welds, as shown in Figure 2. Since the cladding on the spent nuclear fuel inside the WP will degrade unacceptably if heated above 350°C, any heating used for stress relief must be done locally. Other post-weld processing such as peening can also be used to mitigate residual weld stress. Such stress mitigation must also be accounted for in the SCC model.

Predictive Models for SCC. Two alternative SCC models have been considered for application to WP performance assessment. The first (Method A) is the threshold stress intensity factor model for SCC initiation, while the second (Method B) is a variation of the slip-dissolution or film-rupture model for SCC propagation. In the second model, SCC is assumed to initiate if the tensile stress at the smooth surface exceeds a threshold stress.

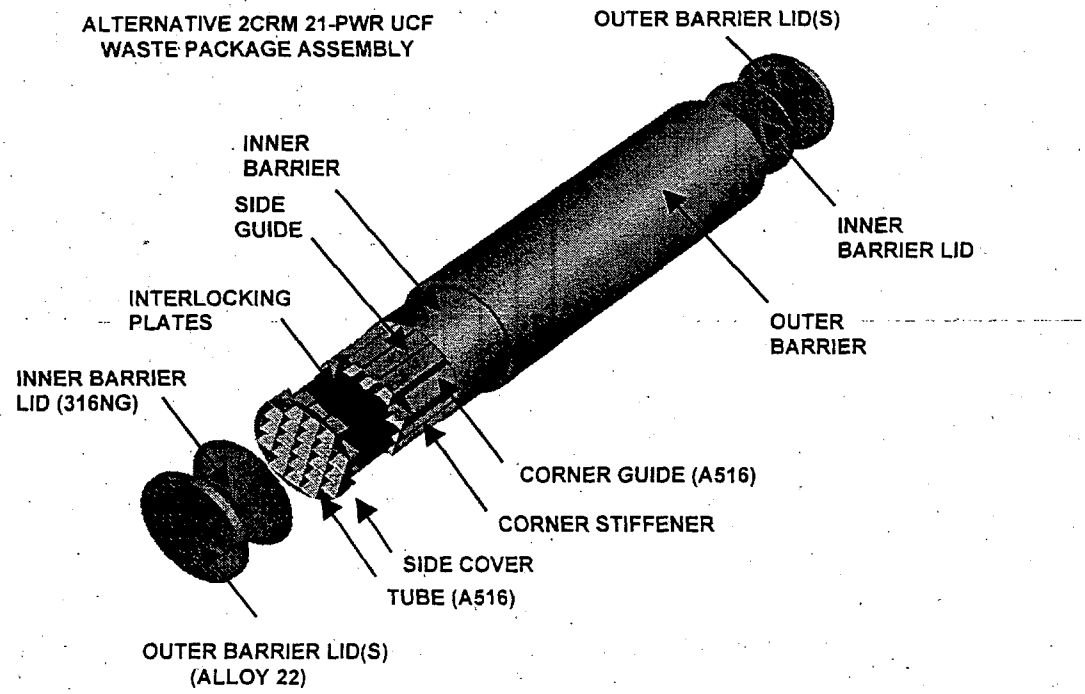

Figure 1. Schematic Representation for CRM 21 WP Design

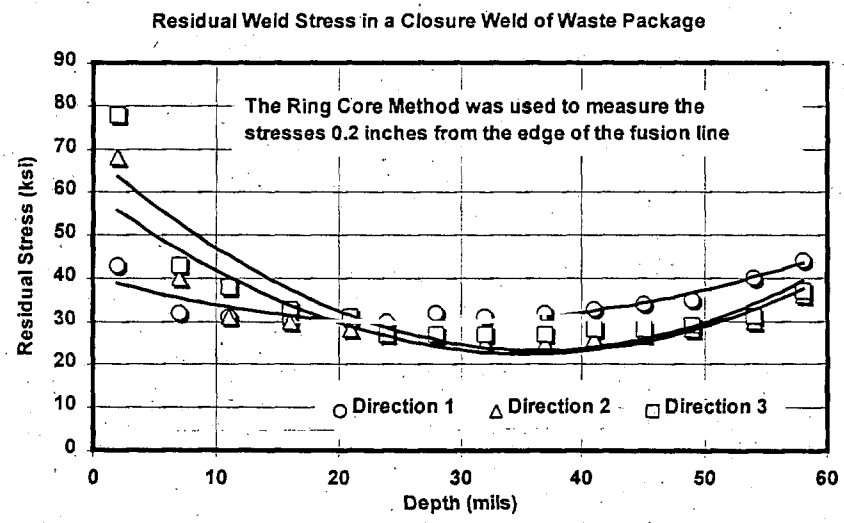

Figure 2. Measured Stress in Alloy 22 Weld

Method A assumes that SCC initiates at pre-existing surface flaws if the stress intensity factor at that flaw (K_I) exceeds the threshold stress intensity factor (K_{ISCC}). If this criterion is not met, no crack will initiate and grow. The K_{ISCC} concept has been widely used by engineers to assess the susceptibility of various materials to SCC. Early SCC tests of Alloy 22 conducted at Lawrence Livermore National Laboratory (LLNL) were based upon this concept. Similar tests have been performed with titanium-based alloys and stainless steels. Predictions based upon this model and preliminary data indicate that circumferential SCC at the final closure weld of the WPOB will be arrested (outer lid). The mean value of K_{ISCC} is greater than the maximum value of K_I estimated for a circumferential flaw in the outer surface. The mean value of K_{ISCC} is 33 MPa $m^{1/2}$ for the outer lid, and 21 MPa $m^{1/2}$ for the inner lid. The maximum value of K_I is 22 MPa $m^{1/2}$ for a circumferential flaw in the outer-lid closure weld, and 13 MPa $m^{1/2}$ for the inner-lid closure weld. The same is true for the closure weld in the underlying structural support (inner lid). Though no circumferential SCC is predicted, through-wall radial cracking does appear to be a possibility.

Method B relates crack propagation (advance) to the periodic rupture and repassivation of the passive film at the crack tip. This approach has been successfully applied to assess SCC crack propagation in light-water nuclear reactors. This model has now been adopted to assess the SCC susceptibility of the materials to be used for the DS and WP. Parameters in this particular model are being quantified through in situ measurements of crack velocity at known stress intensities. Calculated values of K_I indicate eventual penetration of the WPOB closure weld by through-wall radial cracks (which are driven by circumferential tensile forces).

The SCC models are integrated into a larger and more comprehensive model. As discussed in the companion paper on corrosion of the WPOB, the integrated model includes several sub-models to account for dry oxidation (DOX), humid air corrosion (HAC), general corrosion (GC) in the aqueous phase, and localized corrosion (LC) in the aqueous phase. All of these process-level models are abstracted so that they can serve as feeds to the waste package degradation (WAPDEG) code for performance assessment.

Mitigation of Stresses in Closure Weld. Since analyses based on either SCC model (Method A or B) indicate that through-wall radial cracking is a likely threat to the WP, it is necessary to implement post-weld stress mitigation processes at the final closure weld to lower the probability of SCC. As previously discussed, two general approaches have been identified for localized treatment of the closure weld region. One of these involves use of induction coils for localized heating (annealing) of the weld region. The process is conducted as follows:

1. The weld is heated to 1000-1120°C for 30 seconds.
2. The weld is then cooled to a temperature below 500°C during a period of approximately 10 minutes.
3. Surface compression is achieved.

This process has been successfully implemented to lower the residual stress in girth welds of solid-fuel rocket casings with 6-foot diameters. By removing residual tensile stress deep into the weld, SCC could be delayed for long periods of time. However, there are potential problems with this technique. For example, tensile stress may be moved from the weld to an adjacent region, thereby making the adjacent region vulnerable to SCC. A second concern is that the process might heat the WP or contents to unacceptably high temperature. Both possibilities have been analyzed using a detailed finite-element model based on the ANSYS code. The results of such calculations have now shown that localized induction annealing (LIA) is a viable approach.

The second method is known laser peening (LP). In this process, a high-power pulsed laser beam is used to introduce shock waves into the weld surface. These pulses produce compressive stress that counter balances the tensile stress caused by welding (due to shrinkage during cooling). Single-pass LP has been successfully demonstrated on prototypical Alloy 22 welds. Multiple-pass LP can be used to increase the depth of the compressive stress layer. As discussed in a subsequent section, compressive stress can be produced at depths of 2 to 3 mm.

Post-weld stress mitigation processes have a generic shortcoming. The compressive surface layer delays SCC initiation, but does not preclude SCC for all time. Below the layer of compressive stress, the weld region is still under tension. After the compressive layer is lost by corrosion, SCC can initiate in the underlying material.

STRESS ANALYSIS MODEL

Computer Software for Stress Analysis. The computer program known as ANSYS (Version 5.3) was used to calculate weld-induced residual stress, shrink-fit stresses, and the corresponding stress intensity factors in the WP materials. Determining the weld-induced residual stress and the shrink-fit stress is a problem that can best be solved using finite element models. The mesh used to model the WP weld is shown in Figure 3, with various WP cross sections of interest illustrated in Figure 4.

Residual Weld Stress. As seen in Figure 2, significant stress can be introduced into Alloy 22 during welding operations. In evaluating weld-induced stress, the effect of each weld pass is determined by simulating the heat being deposited by the welding process through heat generation rate that is deposited over a prescribed time interval. Typical parameters for weld application include the rate of electrical energy input, the speed of welding, and the assumed efficiency of heating (dependent upon heat transfer). Such information was used to determine the heat generation rate for the elements that represent each weld bead. More on the analysis of residual stress at the closure weld can be found in another paper at this conference entitled *Weld Residual Stress Analyses of Closure Lid Welds for the Waste Packages at the Potential Yucca Mountain Repository* (Tang et al. 2000).

Shrink Fit Stress. The shrink-fit stress analysis was also performed using the ANSYS finite element model. The selected interference fit corresponds to that which causes a stress of one-third of the yield strength (YS) of the material. This interference was determined to be 0.0018 inches at 33% YS.

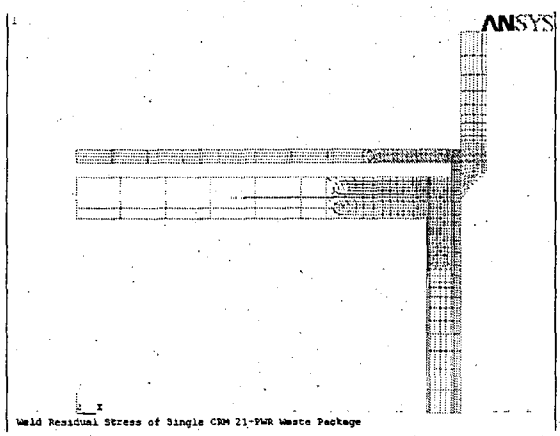

Figure 3. Finite element model for CRM-21 WP

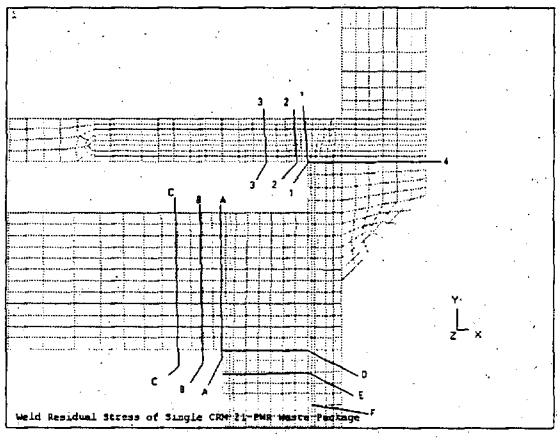

Figure 4. Selected cross-sections for CRM-21 WP design

Stress Intensity Factor Calculation. Both SCC models (Methods A and B) require knowledge of the stress intensity factor (K_I) as a function of crack depth. The calculation of this quantity from the stress distribution in the final closure weld is discussed in this section. Two orientations of the crack (or flaw) relative to the circular closure weld are considered: parallel to the weld (circumferential); and perpendicular to the weld (radial). A flaw with radial orientation is driven by hoop stress, while a flaw with circumferential orientation is driven by radial stress. In either case, the stress intensity factor K_I is defined as a function of stress (σ) and crack depth (a):

$$K_I(a,\sigma) = \beta\sigma\sqrt{\pi a} \qquad \text{(Eq. 1)}$$

where β is a factor dependent on the shape (geometry) of the crack and the configuration of the structural component, and σ is the tensile stress. In most cases of practical importance, closed-form solutions are not available for evaluating K_I since the stress σ may be non-uniformly distributed, and since the geometry factor β is a function of crack size. Closed-form solutions are possible in some ideal cases involving uniform tensile stress and simple geometry, such as the classical problem of a single-edge cracked plate with thickness h. In this case, it has been shown that β can be expressed by the following approximate formula (Ewalds & Wanhill 1984):

$$\beta = 1.12 - 0.231\left(\frac{a}{h}\right) + 10.55\left(\frac{a}{h}\right)^2 - 21.72\left(\frac{a}{h}\right)^3 + 30.95\left(\frac{a}{h}\right)^4 \qquad \text{(Eq. 2)}$$

Since stresses are non-uniformly distributed in most practical problems, the stress intensity factor has to be calculated through application of numerical algorithms (finite element model).

The method discussed here requires that the true value of K_I be calculated from the idealized single-edge cracked plate (SECP) solution through application of a geometry correction factor G. The geometry correction factor is not a constant, but a function of the crack size. The true value of K_I is determined with Equation 3:

$$K_I = G\left(K_I\right)_{SECP} \qquad \text{(Eq. 3)}$$

where $(K_I)_{SECP}$ is the SECP solution for the stress intensity factor. The stress intensity factor for an SECP with an infinitely long flaw is defined by Equation 4 (Buchalet & Bamford 1976).

$$(K_I)_{SECP} = \sqrt{(\pi a)}\left[A_0 F_1 + \left(\frac{2a}{\pi}\right)A_1 F_2 + \left(\frac{a^2}{2}\right)A_2 F_3 + \frac{4a^3}{3\pi}A_3 F_4\right] \qquad \text{(Eq. 4)}$$

where F_0, F_1, F_2 and F_3 are magnification factors. These magnification factors are functions of crack aspect ratio (a/h), where (a) is the crack depth and (h) is the crack thickness (Buchalet & Bamford 1976). The parameters A_0, A_1, A_2 and A_3 are coefficients of a third-order polynomial fit to the through-wall stress distribution. This polynomial is given as Equation 5.

$$\sigma = A_0 + A_1 x + A_1 x^2 + A_1 x^3 \qquad \text{(Eq. 5)}$$

where x is the distance from the outer surface of the closure lid.

Calculated values of K_I for radial elliptical cracks in the outher lid (driven by circumferential tensile force) are shown in Figures 5 and 6, whereas values of K_I for full-circumference crack (driven by radial tensile force) are shown in Figures 7 and 8. In all cases, the crack is assumed to be elliptical with and aspect ratio of 0.5. The curves with *box* symbols account for wall thinning by general corrosion, whereas the curves with *diamond* symbols do not. No post-weld stress mitigation was assumed in this simulation. These values of KI serve as primary inputs to the SCC initiation and propagation models discussed in the following section.

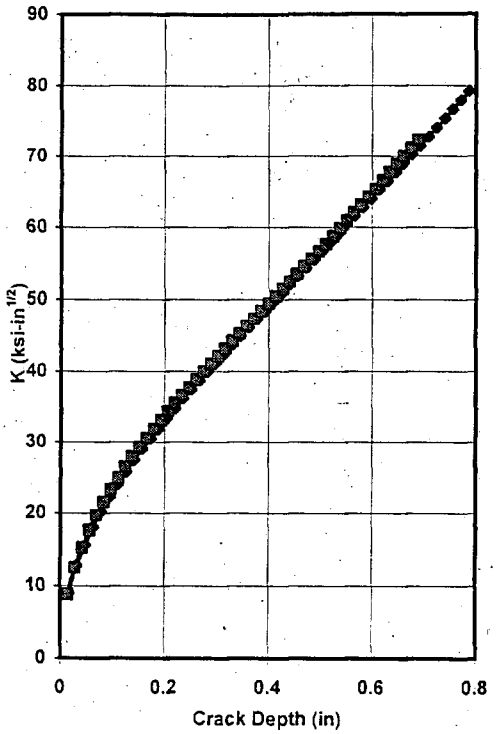

Figure 5. Stress Intensity Factor vs. Crack Depth for Radial Elliptical Crack in Outer Lid

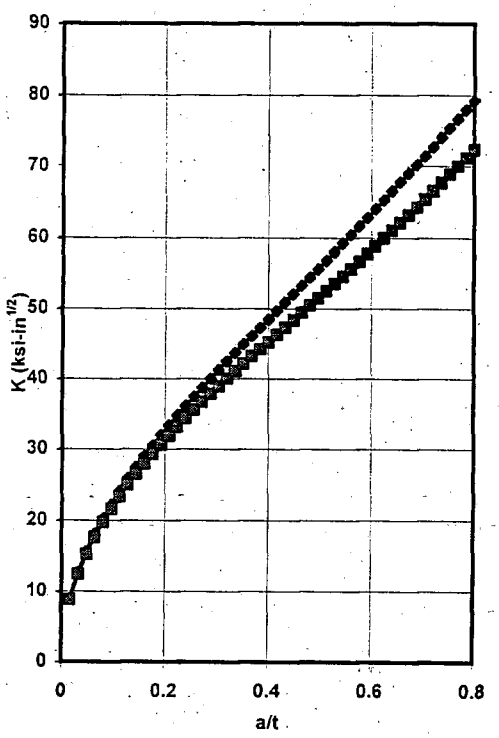

Figure 6. Stress Intensity Factor vs. Normalized Depth for Radial Elliptical Crack in Outer Lid

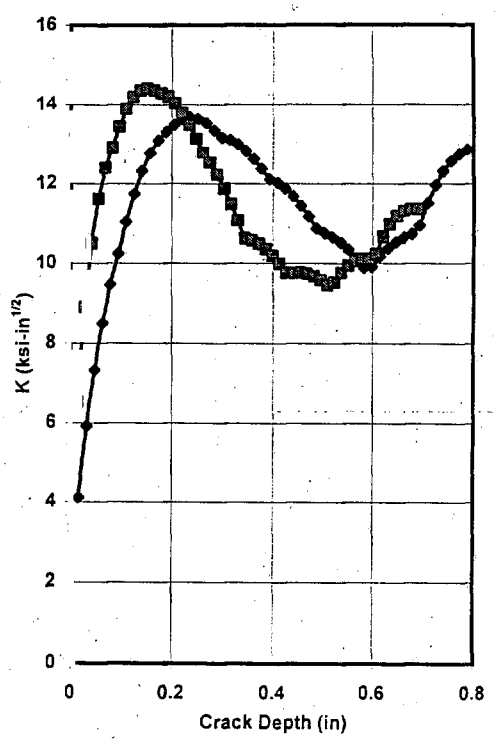

Figure 7. Stress Intensity Factor vs. Crack Depth for Full-Circumference Crack in Outer Lid

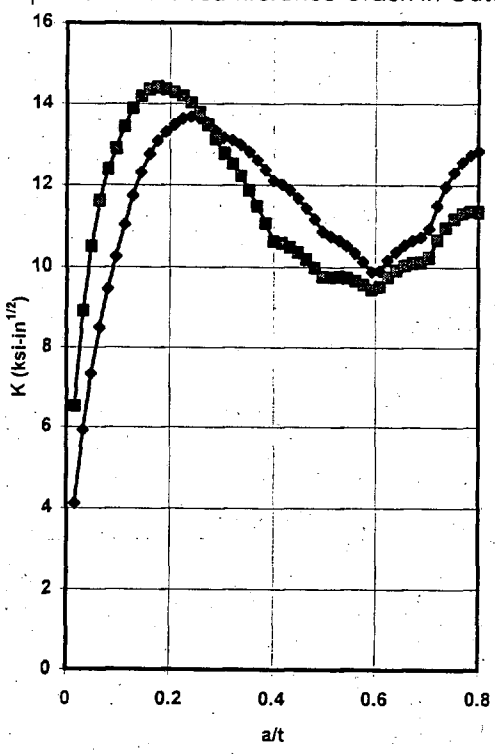

Figure 8. Stress Intensity Factor vs. Normalized Depth for Full-Circumference Crack in Outer Lid

TWO ALTERNATIVE MODELS FOR SCC

Model A – SCC Threshold Model. Method A assumes that SCC initiates at pre-existing surface flaws if the stress intensity factor at that flaw (K_I) exceeds the threshold stress intensity factor (K_{ISCC}). If this criterion is not met, no crack will initiate and grow. The criterion is represented by Equation 6.

$$K_I \geq K_{ISCC} \qquad \text{(Eq. 6)}$$

K_{ISCC} is a material and environment dependent property; which can be obtained through fracture mechanics testing of the materials in the specified environment. The K_{ISCC} concept has been widely used by engineers to assess the susceptibility of various materials to SCC. Descriptions of this concept can be found in Jones and Ricker (1987) and Sprowls (1987).

Values of K_{ISCC} were determined experimentally with wedge-loaded precracked double cantilever beam (DCB) specimens of Alloy 22 and Titanium Grade 12 in deaerated acidic brine at pH ~2.7 and 90°C (Roy et al. 1999). Duplicate samples of each material were loaded at four initial values of the stress intensity factor (K_I), ranging from 20 to 39 ksi $in^{1/2}$ (18 to 35 MPa $m^{1/2}$). Both metallography and compliance methods were used to determine the final crack length. The final stress intensity factor (K_f) was computed from the measured final wedge load on the DCB specimens and the average crack length. This quantity is interpreted as the SCC threshold, K_{ISCC}, although it may only represent an upper bound of the threshold value. Values of K_f for the eight Alloy 22 specimens are 27.96, 28.73, 28.78, 29.58, 29.66, 30.94, 31.98 and 32.39 ksi $in^{1/2}$. If a normal distribution is assumed, the mean value ($K_{ISCC}|_{MEAN}$) and the standard deviation ($K_{ISCC}|_{SIGMA}$) can be calculated:

$$(K_{ISCC}|_{MEAN}) = 30.00 \text{ ksi } in^{1/2} \text{ or } 33.00 \text{ M Pa } m^{1/2}$$

$$(K_{ISCC}|_{SIGMA}) = 1.61 \text{ ksi } in^{1/2} \text{ or } 1.77 \text{ M Pa } m^{1/2}$$

In this initial model, test results for Titanium Grade 12 are assumed to be applicable to both Titanium Grade 7 and 316NG stainless steel. This assumption must be verified in the future with additional test data. Such testing is now underway at LLNL and elsewhere.

In conclusion, the mean values of K_{ISCC} are 33 MPa $m^{1/2}$ for the Alloy 22 outer lid and 21 MPa $m^{1/2}$ for the 316NG inner lid. The maximum values of K_I calculated for circumferential flaws in the closure welds of the outer and inner lids are 22 MPa $m^{1/2}$ and 13 MPa $m^{1/2}$, respectively. Since the mean values of the threshold stress intensity factor (K_{ISCC}) are less than the stress intensity factors associated with circumferential flaws (K_I), SCC initiation at these flaws does not appear to be a significant concern. However, the maximum value of K_I calculated from the hoop stress in the closure weld of the outer lid (80 MPa $m^{1/2}$) does exceed the threshold (33 MPa $m^{1/2}$). Thus, radial cracking is perceived as a potential threat. A similar conclusion is drawn from results for the inner lid.

Model B – Slip Dissolution Model. The theory of slip dissolution (or film rupture) has been successfully applied to assess the SCC crack propagation for light-water nuclear reactors operating at relatively high temperature (~316°C) (Andresen et al. 1994). The slip-dissolution or film-rupture model is discussed in detail in other publications. This model has been adopted to assess the SCC susceptibility of the materials to be used for construction of the DS and WP (Farmer et al. 1991). The ultimate validity of this model and the associated model parameters will be demonstrated and determined through experimental testing at LLNL and elsewhere. It is desirable to separate the SCC mechanism into initiation and propagation phases, though the distinction between these two phases is blurred in experiments. Practical detection of SCC initiation usually requires a crack length of at least a few millimeters (significant metallurgical dimension). The actual initiation step may occur prior to any such detection.

Initiation of embryonic cracks may occur at microscopic surface flaws or sites of localized corrosion (pitting and inter-granular attack). The coalescence of the embryonic cracks to form larger cracks must also be understood. It has been observed that the crack growth rate increases as small cracks coalesce, and approaches a steady-state value when the mean crack length (depth) is about 20 to 50 microns. Thereafter, the crack propagation rate may be analyzed in terms of linear elastic fracture mechanics, normally applicable to long (deep) cracks.

Application of Method B to Nuclear Reactor. Method B has been successfully employed to predict crack extension in boiling-water nuclear reactors (Andresen et al. 19xx). The slip dissolution is represented by Equation 7, which shows the dependence of crack propagation rate (V_t) on the crack tip strain rate ($\dot{\varepsilon}_{ct}$):

$$V_t = A\left(\dot{\varepsilon}_{ct}\right)^n \qquad \text{(Eq. 7)}$$

The parameters A and n depend upon the material and environment at the crack tip. These two parameters can be determined from the measured rate of repassivation. Such measurements are made by rapidly straining wires that are fabricated from the material of interest. The initial application of the slip-dissolution or film-rupture model was on the quantitative prediction of cracking in type 304 or 316 stainless steels in high-purity water at 288°C (boiling-water reactor environment). These investigations led to a quantification of parameters in the model. The value of A is determined with Equation 8:

$$A = 7.8\times10^{-3}(n)^{3.6} \qquad \text{(Eq. 8)}$$

Equations 7 and 8 have been combined to yield Equation 9:

$$V_t = 7.8\times10^{-3}(n)^{3.6}\left(\dot{\varepsilon}_{ct}\right)^n \qquad \text{(Eq. 9)}$$

where V_t has the unit of cm s^{-1} and $\dot{\varepsilon}_{ct}$ has the units of s^{-1}. The exponent n (~0.75) is fundamentally related to the crack tip environment (pH, potential, anionic activity) and material properties. In the case of constant load, the crack-tip strain rate in Equation 9 is related to the engineering stress or the stress intensity factor through Equation 10:

$$\dot{\varepsilon}_{cr} = 4.1\times10^{-14} K_I^4 \qquad \text{(Eq. 10)}$$

where K_I is the in the units of MPa $m^{1/2}$. Substitution of Equation 10 for constant load into Equation 9 yields the following alternative expression for SCC propagation rate:

$$V_I = \overline{A}(K_I)^{\overline{n}} \qquad \text{(Eq. 11)}$$

where

$$\overline{A} = A\left(4.1\times10^{-14}\right)^n \qquad \text{(Eq. 12)}$$

and

$$\overline{n} = 4n \qquad \text{(Eq. 13)}$$

Integration of this crack velocity algorithm is straightforward and leads to an appropriate equation for crack length (depth) as a function time. This approach involves the implicit assumption of an intrinsic initiating defect that exists at time zero. The size of this defect is estimated to be approximately 51 microns (0.002 inches) and would exist on an otherwise smooth surface.

Extension of Method B to Waste Package. It is believed that the SCC of WP materials occurs by the same mechanism that controls SCC of stainless steel in high-temperature BWR environments. The slip-dissolution (or film-rupture) model requires knowledge of two fundamental parameters, the crack-tip strain rate ε_{cr} and the repassivation slope n. The parameter n is an embodiment of the repassivation kinetics, and depends on both the material and the environment. The crack-tip strain rate formula developed for type 316 stainless steel in high-purity water at 288°C is used here for Alloy 22. The value of n for a material known to be highly resistant to SCC is expected to be approximately 0.75. This value is appropriate for making preliminary predictions in the absence of sensitization, at a pH of approximately ten, and in the presence of a balanced collection of anions. Sensitization can have a profound effect on the repassivation kinetcs of stainless steels. Sensitization leads to the precipitation of $Cr_{23}C_6$ at grain boundaries, which is accompanied by the depletion of chromium near the precipitates. Chromium depletion decreases the stability of the passive Cr_2O_3 film. Ongoing and planned experimental activities at LLNL are designed to provide a data base for quantifying the parameters A and n of the slip-dissolution/film-rupture model.

IMPACT OF CORROSION

Calculations were performed using the full thickness for all the WP components (as-built condition). In order to simulate the effect of wall thinning caused by general corrosion, a layer of mesh elements were removed from the outside surface of the outer lid. The thickness of this layer of mesh elements is 0.125 inches, equivalent to 12.7% of the wall thickness. Based on the general corrosion rates for the Alloy 22 (0.05 to 0.731 μm y^{-1}), the time required to remove 12.7% of the container wall will be somewhere between 4,300 and 63,500 years.

This can be simulated with the ANSYS computer program by assigning a death status to the elements representing the outer surface. Removal of these elements causes a redistribution of the stress. ANSYS performs this redistribution to the new equilibrium condition.

Figures 5 through 8 show K_I as a function of distance from the outside surface for circumferential and radial cracks. These figures demonstrate that the overall effect of general corrosion on K_I is small, but does make K_I slightly higher. General corrosion causes thinning of the wall.

The process of SCC is frequently discussed in forms of initiation (incubation and nucleation) and propagation (growth). However, there may be a gradual transition from localized corrosion to crack initiation and growth with no separation of stages, or there may be a repeated succession of short steps of initiation and growth. In any event, from an engineering standpoint, it is convenient to hypothesize the process in two generic stages, initiation and propagation. The initiation of SCC may be due to localized breakdown of the passive film, which can lead to formation of corrosion pits and stress concentration. Thus, the initiation phase is dominated by electrochemical phenomena. In contrast to initiation, propagation is characterized by the growth of relatively large cracks via processes that are dominated by mechanical forces.

ESTIMATE OF CRACK OPENING

Radionuclide release can occur if a crack propagates through the thickness of the container wall. Ultimately, comprehensive finite element analyses should be used to estimate the exact sizes of crack openings. However, a simplified approach has been employed in the initial model. The following assumptions are made for the simplified crack-opening model:

1. A crack) in the outer surface of the closure weld is either circumferential (perpendicular to the radial stress) or radial (perpendicular to the hoop stress).

2. The crack length $2c$ of a circumferential crack remains unchanged as the depth a of the crack grows, while the length of a radial crack will reach the width of the weld as the crack depth grows to the thickness of the container wall.

3. The crack opening has an elliptical shape with length $2c$ and a gap δ.

Tada et al. (1973) has shown that the opening of a crack (δ) in an infinite sheet with plane stress conditions can be calculated with Equation 15.

$$\delta = \frac{(4c)\sigma}{E} \qquad \text{(Eq. 15)}$$

where $2c$ is the length of the crack, σ is the stress and E is Young's modulus. The opening area for an elliptical crack (A_{cr}) is then estimated with Equation 16.

$$A_{cr} = \tfrac{\pi}{4}\delta(2c) = \frac{(2\pi c^2)\sigma}{E} \qquad \text{(Eq. 16)}$$

When Equations 15 and 16 are used to estimate the crack opening and opening area, σ is the maximum stress across the thickness of either the radial stress (for a

circumferential crack) or the hoop stress (for a radial crack).

POST-WELD STRESS MITIGATION

As previously mentioned, two methods have been identified for localized treatment of the closure weld region. The first method involves the laser peening process, where a high powered laser beam is used to introduce shock pulses into the material surface (Figure 9). These pulses introduce compressive stress into the near-surface region. In a single pass, this process is capable of producing compressive layers in Alloy 22 welds at depths of 40 to mils (1 mm). In multiple-pass application, compressive layers can be produced at depths of 120 mils (3 mm). Figures 10 and 11 show the distributions of stress produced in Alloy 22 during single-pass laser peening.

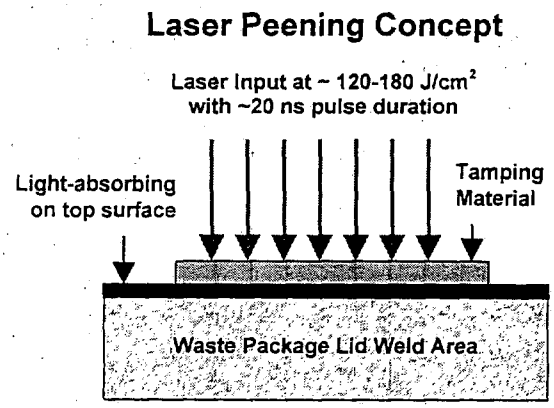

Figure 9. Illustration of laser peening process for stress mitigation

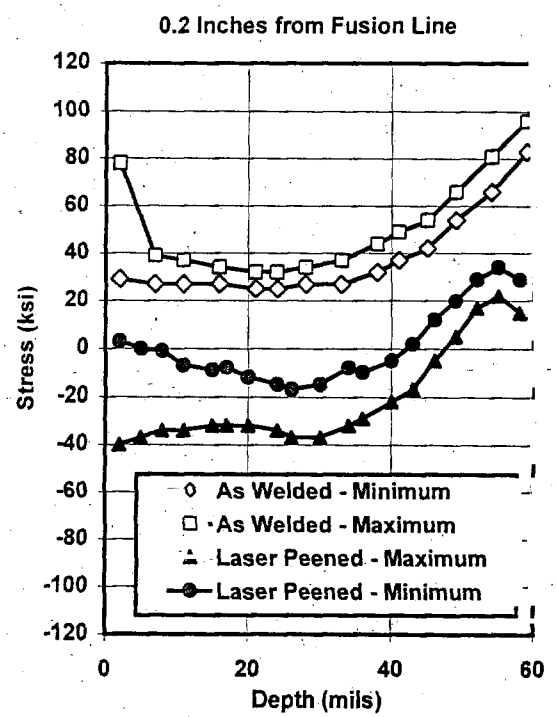

Figure 10. Residual Weld Stress in Alloy 22 at Position 0.2 Inches from the Fusion Line

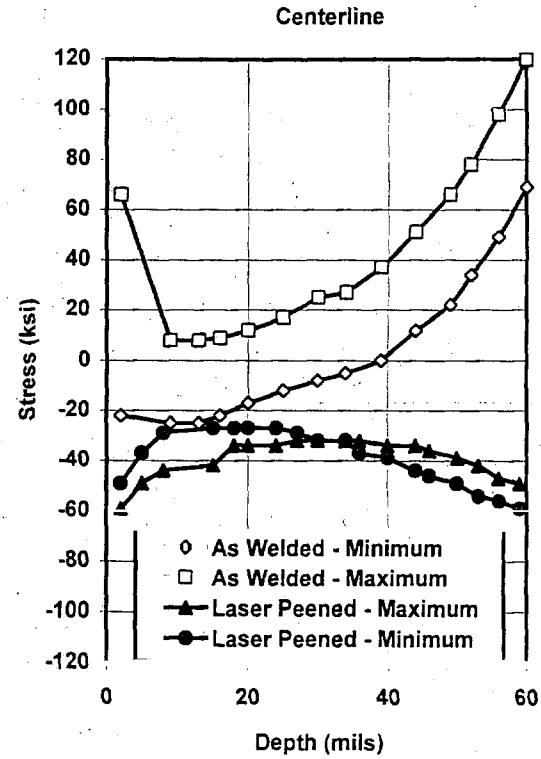

Figure 11. Residual Weld Stress in Alloy 22 at the Center of the Fusion Line

The second post-weld stress mitigation process involves use of induction heating coils to effect localized annealing of the weld region. This process has been used for localized annealing of girth welds in solid-fuel rocket casings with 6-foot diameters. In this case, the residual tensile stresses were successfully neutralized. This process should be able to mitigate residual tensile stress at sufficient depth in the WP closure weld so that SCC initiation is significantly delayed. However, there are some unresolved issues associated with this approach. For example, the process may shift the location of the tensile stresses to a region adjacent to the closure weld, making that region vulnerable to SCC. There is some concern that such a process might heat waste inside the container to unacceptably high temperature. Temperatures above 350°C may damage the cladding on spent nuclear fuel. ANSYS has been used to evaluate both possibilities. The results of this evaluation indicate that localized induction annealing is a viable approach for post-weld mitigation of residual tensile stress. The simulation indicates that the entire surface of the weld can be placed in compression, as shown in Figures 12 and 13. Steps involved in localized induction annealing are summarized as follows:

1. The weld is heated to 1000-1120°C for 30 seconds.
2. The weld is then cooled to a temperature below 500°C during a period of approximately 10 minutes.
3. Surface compression is achieved.

Welding techniques that produce low residual stress are being evaluated.

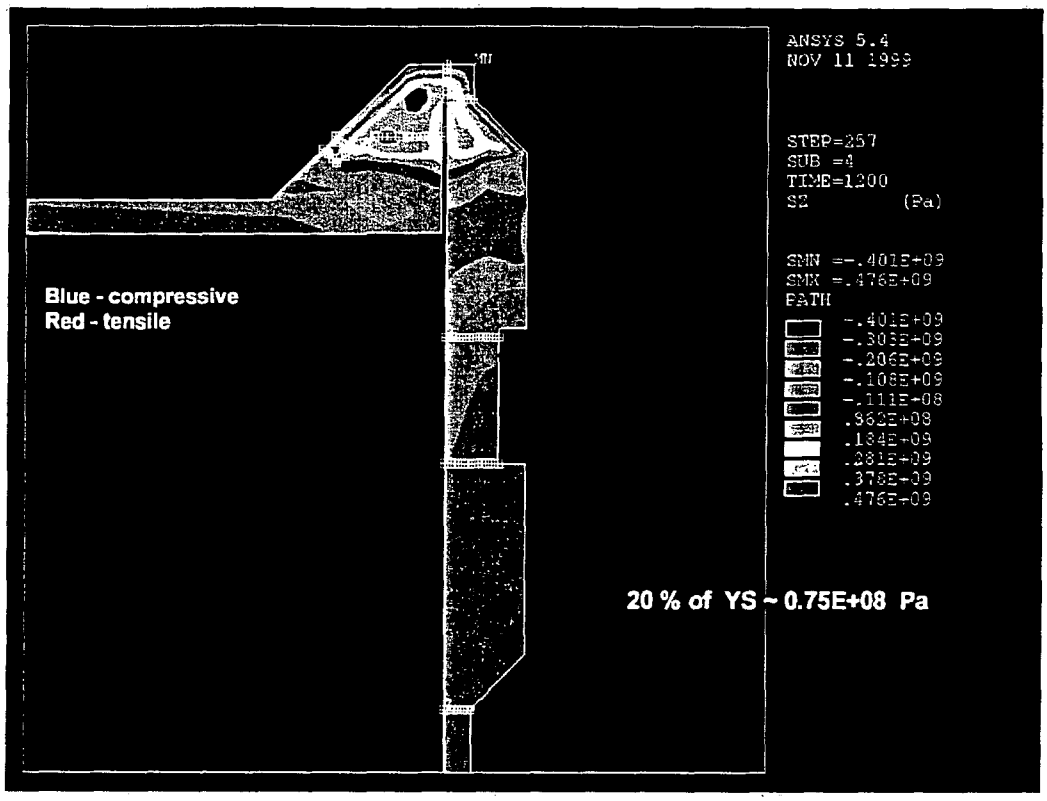

Figure 12. Residual Weld Stress in Alloy 22 at the Center Line

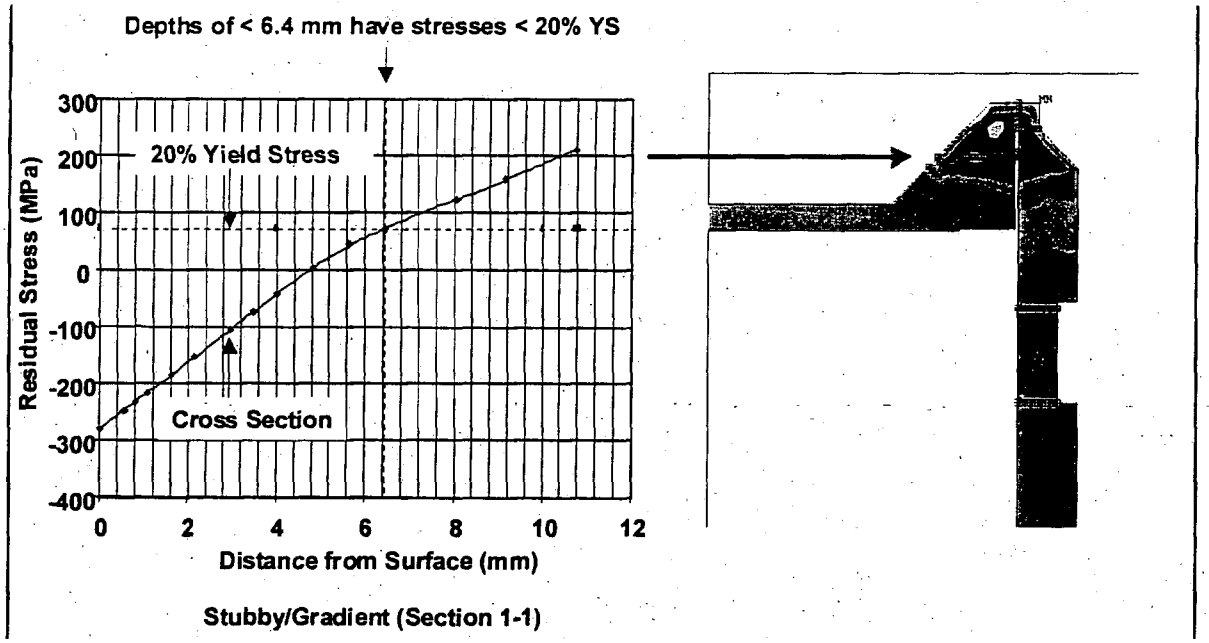

Figure 13. Residual Weld Stress in Alloy 22 at the Center Line

WASTE PACKAGE LIFE

Post-weld stress mitigation should be used to neutralize residual tensile stress in the final closure weld of the WP. The life of the WP will then be determined by the time required to loose the compressive layer by general corrosion or some other means. Figure 14 shows penetration as a function of time for Alloy 22, based upon an experimentally-determined cumulative distribution function (CDF) for general corrosion rates (Figure 52, Table 26, Farmer 2000). Lines are given for various percentiles of the CDF. The three horizontal lines labeled as Mitigation 1, Mitigation 2 and Mitigation 3 correspond to hypothetical cases where post-weld stress mitigation has been used to introduce near-surface compression at depths of 1, 3 and 5 mm, respectively. The intersection these horizontal lines with those representing WP penetration due to general corrosion (CDF for general corrosion rate) determine the time required for initiation of SCC. The time required for initiation is roughly equivalent to the time at which the WP is expected to fail. This figure is an illustration of the factors that control failure of a weld by SCC after post-weld stress mitigation and is not intended as any formal estimate of performance assessment.

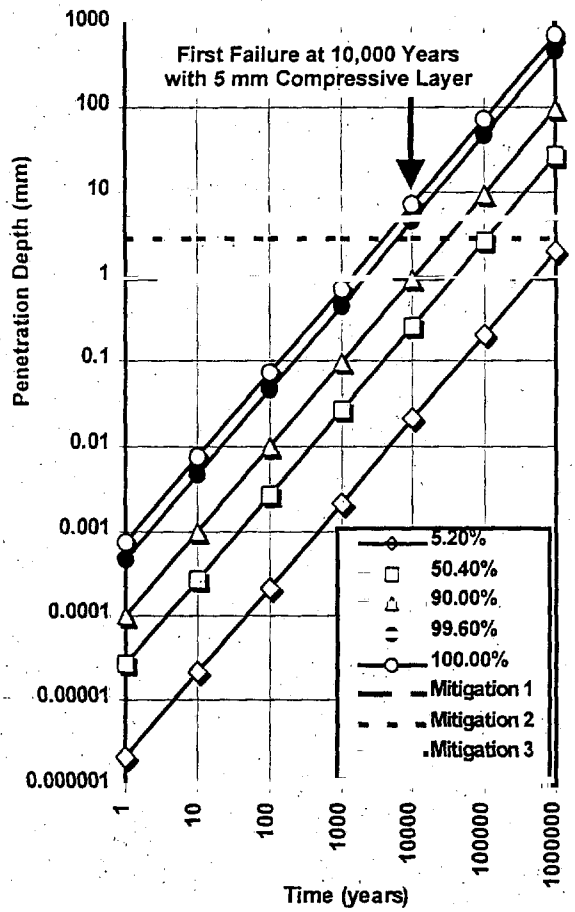

Figure 14. Determination of Waste Package Life from Compressive Layer Thickness and Penetration Due to General Corrosion (Alloy 22)

CONCLUSIONS

There are several modes of failure that could lead to premature breach of the waste package. One of the most threatening is stress corrosion cracking (SCC). Initiation and propagation of SCC can occur at relatively low stress intensity factors (K_I). After initiation, through-wall penetration is essentially instantaneous when compared to the 10,000-year time scale of importance to the high-level waste repository at Yucca Mountain. Three criteria have to be met for SCC to occur: metallurgical susceptibility; a corrosive environment; and static tensile stresses. Environments that cause SCC are usually aqueous and can be condensed layers of moisture or bulk solutions. The SCC of a particular alloy is usually caused by the presence of a specific chemical species in the environment. For example, the SCC of copper alloys is virtually always due to the presence of ammonia in the environment. Chloride ions cause SCC in stainless steels and aluminum-based alloys. Reduced sulfate is known to promote SCC in nickel-based alloys. Changes in the environmental conditions, which include temperature, dissolved oxygen, and ionic concentrations, will normally influence the SCC process.

Environmental conditions believed to be relevant to Yucca Mountain are described in the companion paper entitled *General and Localized Corrosion of Outer Barrier of High-Level Waste Container in Yucca Mountain.* Plausible conditions are represented by several standardized test media which include simulated dilute water (SDW), simulated concentrated water (SCW), simulated acidified water (SAW), simulated saturated water (SSW), and basic saturated water (BSW). These solutions are based upon the concentration of J-13 well water (Harrar et al. 1999).

Radionuclide release is possible if SCC causes breach of the WPOB and underlying structural support. Adequate models to account for SCC must therefore be employed. As will be discussed subsequently, the highest stress in the WPOB (and the highest probability of SCC) will be in the final closure weld. Since the cladding on the spent nuclear fuel inside the WP will degrade unacceptably if heated above 350°C, any heating used for stress relief must be done locally. Other post-weld processing such as peening can also be used to mitigate residual weld stress. Such stress mitigation must also be accounted for in the SCC model.

Two alternative SCC models have been considered for application to WP performance assessment. The first (Method A) is the threshold stress intensity factor model for SCC initiation, while the second (Method B) is a variation of the slip-dissolution or film-rupture model for SCC propagation. In the second model, SCC is assumed to initiate if the tensile stress at the smooth surface exceeds a threshold stress. Analyses based upon Method A indicate that radially-oriented stress corrosion cracks may be possible in the final closure weld. The mean values of K_{ISCC} are 33 MPa $m^{1/2}$ for the outer lid (Alloy 22) and 21 MPa $m^{1/2}$ for the inner lid (316NG). The maximum values of K_I for circumferential flaws in the closure welds of the outer and inner lids are 22 MPa $m^{1/2}$ and 13 MPa $m^{1/2}$, respectively. Since the mean values of the threshold stress intensity factor are less than the stress intensity factors

associated with circumferential flaws, SCC initiation at these flaws does not appear to be a significant concern. However, the maximum value of K_I calculated from the hoop stress in the closure weld of the outer weld (80 MPa $m^{1/2}$) exceeds threshold for SCC (33 MPa $m^{1/2}$). A similar conclusion is drawn from results for the inner lid. may be exceeded in the closure welds of either lid.

Method B relates crack propagation (advance) to the periodic rupture and repassivation of the passive film at the crack tip. This approach has been successfully applied to assess SCC crack propagation in light-water nuclear reactors. This model has now been adopted to assess the SCC susceptibility of the materials to be used for the DS and WP. Parameters in this particular model are being quantified through in situ measurements of crack velocity at known stress intensities. Calculated values of K_I indicate eventual penetration of the WPOB closure weld by through-wall radial cracks (which are driven by circumferential tensile forces).

Since analyses based on either SCC model (Method A or B) indicate that through-wall radial cracking is a likely threat to the WP, it is necessary to implement post-weld stress mitigation processes at the final closure weld to lower the probability of SCC. As previously discussed, two general approaches have been identified for localized treatment of the closure weld region. One of these involves use of induction coils for localized heating (annealing) of the weld region. This process has been successfully implemented to lower the residual stress in girth welds of solid-fuel rocket casings with 6-foot diameters. By removing residual, tensile stress deep into the weld, SCC could be delayed for long periods of time. However, there are potential problems with this technique. For example, tensile stress may be moved from the weld to an adjacent region, thereby making the adjacent region vulnerable to SCC. A second concern is that the process might heat the WP or contents to unacceptably high temperature. Both possibilities have been analyzed using a detailed finite-element model based on the ANSYS code. The results of such calculations have now shown that localized induction annealing is a viable approach.

In the laser peening process, a high-power pulsed laser beam is used to introduce shock waves into the weld surface. These pulses produce compressive stress that counter balances the tensile stress caused by welding (due to shrinkage during cooling). Multiple-pass LP can be used to increase the depth of the compressive stress layer. This process has been successfully demonstrated on prototypical Alloy 22 welds. As discussed in a subsequent section, compressive stress can be produced at depths of 2 to 3 mm. Deeper penetration may be possible with multiple-pass LP, but has not yet been demonstrated.

Post-weld stress mitigation processes have a generic shortcoming. The compressive surface layer delays SCC initiation, but does not preclude SCC for all time. Below the layer of compressive stress, the weld region is still under tension. After the compressive layer is lost by corrosion, SCC can initiate in the underlying material.

ACKNOWLEDGEMENTS

Work was sponsored by the U.S. Department of Energy Office of Civilian and Radioactive Waste Management (OCRWM). This work was done under the auspices of the U.S. Department of Energy (DOE) by Lawrence Livermore National Laboratory (LLNL) under Contract No. W-7405-Eng-48.

REFERENCES

Andresen, P. L.; Ford, F. P. 1994. International Journal of Pressure Vessels and Piping **59**, 61-70.

Buchalet, C. B.; Bamford, W. H. 1976. *Mechanics of Crack Growth*, ASTM Special Publication STP 590, pp. 385-402.

Civilian Radioactive Waste Management (CRWMS) Management and Operating Contractor (M&O) 1999. License Application Design Selection (LADS) Report, B00000000-01717-4606-00123 Rev. 01 ICN 01, CRWMS M&O, Las Vegas, Nevada.

Ewalds, H. L.; Wanhill, R. J. H. 1984. *Fracture Mechanics*, Edward Arnold Pty. Ltd. & Delftse Uitgevers Maatschappij.

Farmer, J. C.; Gdowski, G. E.; McCright, R. D.; Ahluwalia, H. S. 1991. Nuclear Engineering Design **129**, 57-88.

Farmer, J. C. 2000. General Corrosion and Localized Corrosion of Waste Package Outer Barrier, CRWMS M&O ANL-EBS-MD-000003 Rev. 0 ICN 0, Las Vegas, Nevada.

Farmer et al. 2000. *General and Localized Corrosion of Outer Barrier of High-Level Waste Container in Yucca Mountain*, ASME PVP Conference, Seattle, Washington.

Harrar, J.E.; Carley, J.F.; Isherwood, W.F.; and Raber, E. 1990. UCID-21867, 111 p.

Jones, R. H.; Ricker, R. E. 1987. *ASM Metals Handbook*, 9th Ed., Vol. 13, pp. 145-163.

Lu, S. 2000. Stress Corrosion Cracking, CRWMS M&O ANL-EBS-MD-000005 Rev. 0 ICN 0, Las Vegas, Nevada.

Sprowls, D. O. 1987. *ASM Metal Handbooks*, 9th Ed., Vol. 13, pp. 245-282.

Summers, T. 2000. Aging and Phase Stability of Waste Package Outer Barrier, CRWMS M&O ANL-EBS-MD-000002 Rev. 0 ICN 0, Las Vegas, Nevada.

Tada, H.; Paris, P.; Irwin, G. 1973. *The Stress Analysis Handbook*, 2nd Ed., Del Research Corporation.

Tang et al. 2000. *Weld Residual Stress Analyses of Closure Lid Welds for the Waste Packages at the Potential Yucca Mountain Repository*, ASME PVP Conference, Seattle, Washington.

Treseder, R. S.; Baboian, R.; Munger, C. G. 1991. NACE Corrosion Engineer's Reference Book, 2nd Ed., 168-170, 178-183.